Kühn, H. (1984) *Prog. Retinal Res. 3*, 123–156.
Kühn, H., Bennett, N., Michel-Villaz, M., & Chabre, M. (1981) *Proc. Natl. Acad. Sci. U.S.A. 78*, 6873–6877.
Laemmli, U. K. (1970) *Nature (London) 227*, 680–685.
Lamola, A. A., Yamane, T., & Zipp, A. (1974a) *Biochemistry 13*, 738–745.
Lamola, A. A., Yamane, T., & Zipp, A. (1974b) *Exp. Eye Res. 18*, 19–27.
Liebman, P. A., & Sitaramayya, A. (1984) *Adv. Cyclic Nucleotide Protein Phosphorylation Res. 17*, 215–225.
Lindmann, B., & Wennerström, H. (1980) *Top. Curr. Chem. 87*, 85–83.
Litman, B. J., Kalisky, O., & Ottolenghi, M. (1981) *Biochemistry 20*, 631–634.
Longstaff, C., Calhoon, R. D., & Rando, R. R. (1986) *Proc. Natl. Acad. Sci. U.S.A. 83*, 4209–4213.
Lühmann, B., & Finkelmann, H. (1986) *Colloid Polym. Sci. 264*, 189–192.
Lühmann, B., & Finkelmann, H. (1987) *Colloid Polym. Sci.* (in press).
Makino, M., Suzuki, T., Ebina, Y., & Nagai, K. (1980) *Biochim. Biophys. Acta 600*, 332–342.
Marquart, D. W. (1963) *J. Soc. Ind. Appl. Math. 11*, 431–441.
Matthews, R. G., Hubbard, R., Brown, P. K., & Wald, G. (1963) *J. Gen. Physiol. 47*, 215–240.
O'Brien, D. F., Costa, L. F., & Ott, R. A. (1977) *Biochemistry 16*, 1295–1303.
Okada, D., Tsukida, K., & Ikai, A. (1985) *Photochem. Photobiol. 42*, 405–411.
Parkes, J. H., & Liebman, P. A. (1984) *Biochemistry 23*, 5054–5061.
Pichat, L., Baret, C., & Audinot, M. (1956) *Bull. Soc. Chim. Fr.*, 151–156.
Schleicher, A., & Hofmann, K. P. (1987) *J. Membr. Biol. 95*, 271–281.
Schmidt, G., & Knoll, W. (1985) *Ber. Bunsen-Ges. Phys. Chem. 89*, 36–43.
Seebach, D., Hungerbühler, E., Naef, R., Schnurrenberger, P., Weidmann, B., & Züger, B. (1982) *Synthesis*, 138–141.
Sengbusch, G. v., & Stieve, H. (1971) *Z. Naturforsch., B: Anorg. Chem., Org. Chem., Biochem., Biophys., Biol. 26b*, 861–862.
Shichi, H., Muellenberg, C. G., Harosi, F. I., & Somers, R. L. (1977) *Vision Res. 17*, 633–636.
Stewart, J. G., Baker, B. N., Plante, E. O., & Williams, T. P. (1976) *Arch. Biochem. Biophys. 172*, 246–251.
Stubbs, G. W., Smith, H. G., & Litman, B. J. (1976) *Biochim. Biophys. Acta 425*, 46–56.
Tanford, C., & Reynolds, J. A. (1976) *Biochim. Biophys. Acta 457*, 133–170.
Welte, W., Wacker, T., Leis, M., Kreutz, W., Shiozawa, J., Gad'on, N., & Drews, G. (1985) *FEBS Lett. 182*, 260–264.
Weltzien, H. U. (1979) *Biochim. Biophys. Acta 559*, 259–287.
Weltzien, H. U., Richter, G., & Ferber, E. (1979) *J. Biol. Chem. 254*, 3652–3657.
Wennerström, H., & Lindmann, B. (1979) *Phys. Rep. 52*, 83–86.
Williams, T. P., Baker, B. N., & McDowell, J. H. (1974) *Exp. Eye Res. 18*, 69–75.

Secondary Structure Determination of Human β-Endorphin by ^{1}H NMR Spectroscopy†

Olivier Lichtarge,‡ Oleg Jardetzky,*,‡ and Choh Hao Li§

Stanford Magnetic Resonance Laboratory, Stanford University, Stanford, California 94305-5055, and Laboratory of Molecular Endocrinology, University of California, San Francisco, California 94143

Received March 11, 1987; Revised Manuscript Received April 16, 1987

ABSTRACT: The ^{1}H NMR spectra of human β-endorphin indicate that the peptide exists in random-coil form in aqueous solution but becomes helical in mixed solvent. Thermal denaturation NMR experiments show that in water there is no transition between 24 and 75 °C, while a slow noncooperative thermal unfolding is observed in a 60% methanol–40% water mixed solvent in the same temperature range. These findings are consistent with circular dichroism studies by other workers concluding that β-endorphin is a random coil in water but that it forms 50% α-helix or more in mixed solvents. The peptide in the mixed water–methanol solvent was further studied by correlated spectroscopy (COSY) and nuclear Overhauser effect spectroscopy (NOESY) experiments. These allow a complete set of assignments to be made and establish two distinct stretches over which the solvent induces formation of α-helices: the first occurs between Tyr-1 and Thr-12 and the second between Leu-14 and extending to Lys-28. There is evidence that the latter is capped by a turn occurring between Lys-28 and Glu-31. These helices form at the enkephalin receptor binding site, which is at the amino terminus, and at the morphine receptor binding site, located at the carboxyl terminus [Li, C. H. (1982) *Cell (Cambridge, Mass.) 31*, 504–505]. Our findings suggest that these two receptors may specifically recognize α-helices.

Because of the wide range of its pharmacological effects, the structure of β-endorphin is of interest. The sequence of this 31 amino acid endogenous opioid peptide, shown in Figure 1, is highly conserved throughout evolution (Li, 1982) and corresponds to the 61–91 C-terminal fragment of the hormone β-lipotropin (Li, 1964). Two of its fragments are also active neuropeptides: Met-enkephalin (Hughes et al., 1975) made up from the first five residues and dynorphin-(1–4) (Goldstein et al., 1979), which consists of the first four residues. β-En-

† This research was supported in part by Grants DA-03434 and GM-02907 from the USPHS to C.H.L. and by NIH Grants RR02300 and RR00711 and NSF Grant DMB84-02348 to O.L. and O.J.
‡ Stanford University.
§ University of California.

0006-2960/87/0426-5916$01.50/0

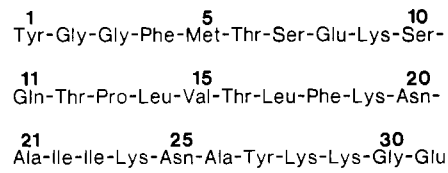

FIGURE 1: Amino acid sequence of human β-endorphin.

dorphin binds to the μ, δ, and κ opioid receptors in the brain, inducing many pharmacological activities such as catalepsia, hypothermia, and sedation (Smith & Loh, 1981; Simon, 1982; Kosterlitz, 1985). There is also evidence for a fourth, highly β-endorphin specific, receptor type: the ε-receptor of the rat vas deferens (Wuster et al., 1979, 1980; Schulz et al., 1981). The binding regions to the δ and μ receptors have been suggested to be the Met-enkephalin segment, Tyr-1–Met-5, and the Ala-21–Gly-31 region, respectively (Li, 1982).

Bewley and Li (1983, 1985) have reported evidence of tertiary structure, but most other studies have focused on the presence of secondary structure. Circular dichroism (CD) studies in water find no significant sign of secondary structure (Hollosi et al., 1977) in agreement with a hydrodynamic study (Yang et al., 1977), but the addition of methanol induces a steady noncooperative conformational transition that could contain as much as 50% α-helix (Yang et al., 1977; Jibson & Li, 1981). Similar helix inductions have been reported in the presence of trifluoroethanol (Hollosi et al., 1977; Graf et al., 1980), sodium dodecyl sulfate (Yang et al., 1977), and various lipids (Wu et al., 1979). The CD spectra from deletion fragments in methanol suggest that the α-helix is induced in the C-terminal region (Jibson & Li, 1981), though Hollosi reported that in trifluoroethanol the fragment from residue 20 to 31 showed little α-helix formation. The ability of these fragments to bind onto rat brain membrane is correlated to their helix-forming potential in trifluoroethanol (Hammonds et al., 1982).

Different groups have applied the Chou–Fasman method to predict the secondary structure and have obtained different results. Wu et al. (1979) find α-helical potential from residues 4 to 11 and 21 to 29 and β-sheet potential between residues 14 and 18. Jibson and Li (1981) find helical potential between residues 4 and 9 and β-sheet potential from residues 14 to 24 with a possible β-turn at residue 25 or 27. Graf et al. (1980) predict the formation of a helix between residues 13 and 29 and of a β-turn between residues 1 and 4. Hammonds et al. (1982) note that a helix from residues 14 to 24 is not only consistent wtih Chou–Fasman criteria but should be especially likely because of its amphiphilic character (and also that β-turns which strictly meet the Chou–Fasman criteria can occur only at the C-terminal end at residues 27–30 or 28–31).

Using a series of synthetic peptides aimed at preserving the amphiphilic characteristics of the potential C-terminal helix of β-endorphin, Kaiser and colleagues (Kaiser & Kezdy, 1984; Taylor et al., 1981, 1982, 1983; Blanc et al., 1983; Blanc & Kaiser, 1984) obtained many peptides with binding characteristics and potencies similar to that of β-endorphin. However, another synthetic peptide designed to be helical but not amphiphilic (Blanc et al., 1983) was also found to be as potent as β-endorphin. These experiments show that a helical potential in the C-terminal region is *sufficient* for binding to the opiate receptors and for opiate activity.

Previous NMR studies on β-endorphin in aqueous solution have shown that the Gly-30 residue, at the C-terminal end, has a chemical shift consistent with a random-coil conformation, while at the N-terminus Gly-2 and Gly-3 have chemical shifts similar to those of Met-enkephalin. These are slightly upfield of the expected random-coil shift due to the local interaction with the neighboring Phe-4 (Cabassi & Zetta, 1982). A set of photochemically induced dynamic nuclear polarization (photo-CIDNP) studies has focused on the effect of phospholipid micelles on the accessibility and mobility of Tyr-1 and Tyr-27 (Zetta et al., 1982, 1983; De Marco et al., 1985). These show that a large percentage of the peptide binds onto the micelle surface. Tyr-1 does retain its mobility though, while Tyr-27 has strongly diminished mobility and accessibility.

This study aims at characterizing the secondary structure of β-endorphin in water and water–methanol. Because conformational changes in a protein are reflected in changes in the NMR spectra, temperature experiments were undertaken in both solvents. In water, no changes were observed, as would be expected in a random coil. But in water–methanol, thermal denaturation was observed, indicating the presence of a nonrandom structure. To characterize it, we applied two-dimensional NMR methods, extensively developed for proteins by Wüthrich and co-workers (Wagner et al., 1981; Wüthrich et al., 1982, 1984; Billeter et al., 1982). These techniques are well suited for the study of peptides (Wemmer & Kallenbach, 1983; Gariepy et al., 1986) and small proteins (Zuiderweg et al., 1983; Williamson et al., 1984; Kline & Wüthrich, 1985; Wemmer et al., 1986; Holak & Prestegard, 1986).

Materials and Methods

Sample Preparation. Human β-endorphin was synthesized by the solid-phase synthesis method as described elsewhere (Li et al., 1977). Samples were prepared with purified or perdeuteriated water and perdeuteriated methyl alcohol (100% D) obtained from Aldrich Chemical Co. In water the pH was adjusted to 1.7 with small aliquots of DCl. The methanol solution was obtained from the lyophilized water solution, and the mixed solvent solution was prepared by dilution with water. The one-dimensional spectroscopy was performed at concentrations of 1 mM, and the two-dimensional (2-D) experiments were performed at 3 mM concentrations. The peptide showed some tendency toward aggregation after long periods of refrigeration, but clear samples were always obtained after moderate warming and shaking.

Data Acquisition. The temperature experiments were performed at 360 MHz on a modified Bruker HXS-360 spectrometer equipped with a Nicolet 1180 data system. Typically, each spectrum was collected with a single pulse experiment with a 90° pulse, a 1–1.5-s pulse delay time, and a total sweep width of 3400 Hz sampled with 8192 points under conditions of homogated decoupling resulting in water presaturation at all times except during acquisition. Data processing was done by using a line-broadening factor of 1 Hz. The spectra were referenced by putting the first upfield tyrosine peak at 6.80 ppm.

The two-dimensional experiments were performed at 500 MHz on a JEOL GX-500 spectrometer. The ^1H correlated spectroscopy (COSY) (Aue et al., 1976a; Nagayama et al., 1980; Bax & Freeman, 1981; Wider et al., 1984), nuclear Overhauser enhancement spectroscopy (NOESY) (Jeener et al., 1979; Anil-Kumar et al., 1980; Wider et al., 1984), and two-dimensional *J*-resolved spectroscopy experiments (Aue et al., 1976b) were all collected in absolute value mode at a temperature of 23 °C with water-peak suppression obtained through continuous irradiation except during acquisition. All spectra were referenced with respect to the residual protonated methanol resonance at 3.30 ppm.

For the COSY, the standard pulse sequence was used ($90–t_1–90–t_2$, where t_1 and t_2 are the evolution and detection periods, respectively), with 1024 points in F2, the second

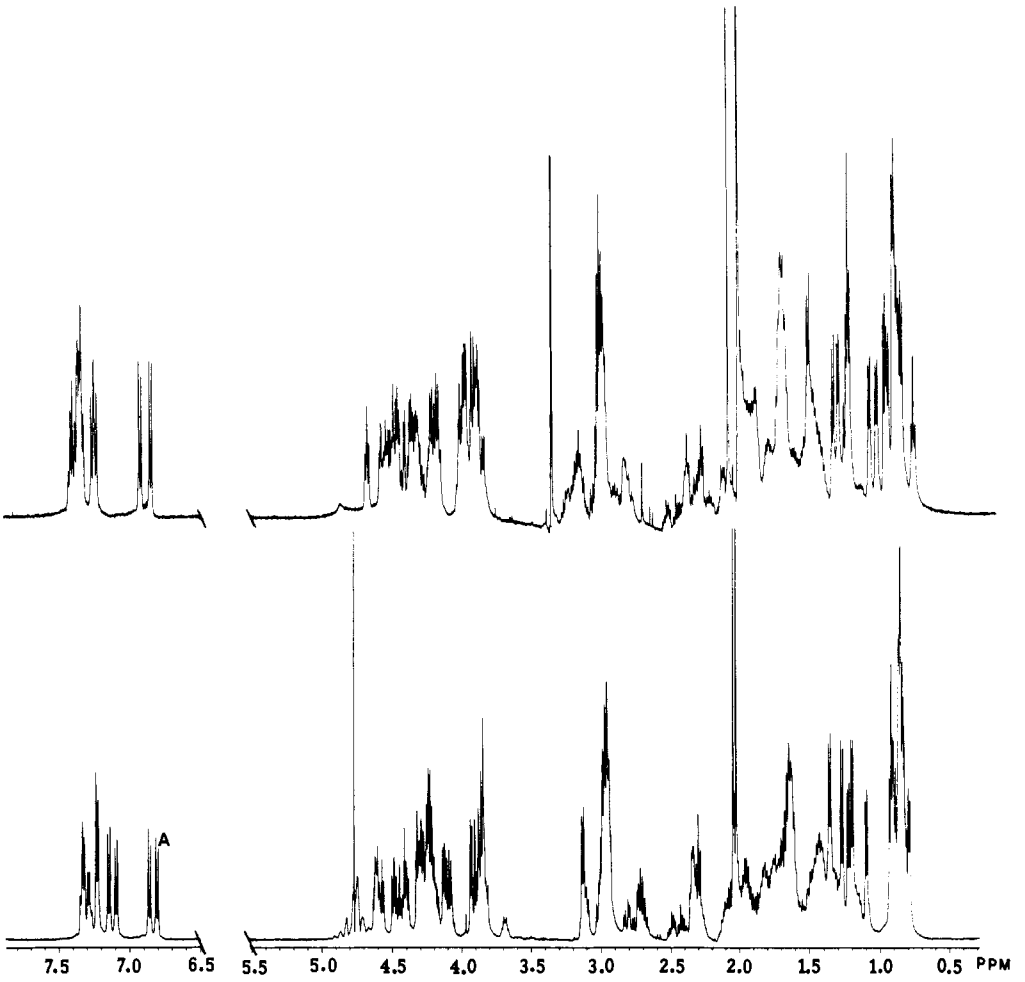

FIGURE 2: ^{1}H NMR (500 MHz) spectra of human β-endorphin in D_2O (bottom) and in 60% CD_3OD–40% D_2O (top). For both spectra T = 23 °C, in water the pH was 1.7, and the reference is set so that tyrosine peak A is at 6.80 ppm. In the mixed solvent the reference is the internal methanol peak at 3.30 ppm.

frequency domain, and 256 points in the first frequency domain F1, later zero-filled to 512 points. Each slice of F1 contained 272 accumulations with a pulse recovery time of 2 s and had a spectral width of 4302.9 Hz. Prior to Fourier transformation, the time domain data matrix was multiplied by a trapezoidal window convoluted with a sine bell. A symmetrization routine was applied to yield a 512 by 512 data matrix in the frequency domain with 8.4-Hz resolution in either direction.

For the NOESY experiments, the standard pulse sequence (90–t_1–90–τ_m–90–t_2, where τ_m is the mixing time) was used, with mixing times of 250, 300, and 400 ms. In the F1 dimension there were 224, 192, and 192 points, respectively, for each mixing time, all later zero-filled to 512 points. The slices for each experiment had 160, 172, and 272 scans, respectively. The pulse recovery times were 4 s for τ_m of 250 and 300 ms, and 3 s for τ_m of 400 ms. In all cases there were 1024 points in F2, sampling a spectral width of 4302.9 Hz. The data processing was similar to that described for the COSY.

The 2-D J-resolved experiment was performed with the standard pulse sequence (90–$t_1/2$–180–$t_1/2$–t_2, where the evolution period t_1 is split by a 180° pulse). In F2, 4096 points were collected for a sweep width of 3882.3 Hz, and along F1 64 points were zero-filled to 128 for a frequency range of 128 Hz. Resolution enhancement in F2 and a line broadening of 1 Hz were applied during the processing.

RESULTS

A temperature series was performed on a sample of human β-endorphin in 100% (deuteriated) water by recording spectra between temperatures of 24 and 80 °C in steps of 9 °C. These spectra were referenced to a tyrosine ϵ-CH peak, fixed to be at 6.85 ppm. A number of easily identifiable peaks were followed. All the chemical shift changes involved were small, at most 0.04 ppm over 66 °C. There is a global upfield trend of the chemical shifts with the temperature increase, suggesting that the reference tyrosine peak is, in fact, moving slightly downfield. The changes in shifts are not entirely smooth, with the most drastic changes occurring between 24 and 35 °C (though even there the greatest change is of −0.03 ppm).

This region of the temperature dependence was explored with more care in a second experiment, in which spectra were recorded between 25 and 35 °C in steps of 2 °C. Particular interest was paid to the α-CH region, which would readily reflect changes in the backbone conformation. However, this experiment also failed to show that a transition to a different conformational state occurred. All of the α-CH resonances varied by less than 0.005 ppm. Similarly, the remainder of the spectra also showed little sign of transition over this range in temperature.

We conclude that no significant change occurs in the β-endorphin spectrum between 24 and 80 °C that could be attributable to a conformational transition.

As can be seen from Figure 2, the spectra in water and in the 60% methanol–40% water mixed solvent are significantly different. Some changes are expected since amino acids have different chemical shifts in different solvents (Jardetzky & Roberts, 1981). However, the detached triplet at 0.75 ppm, which is clearly upfield of the rest of the resonances, is highly

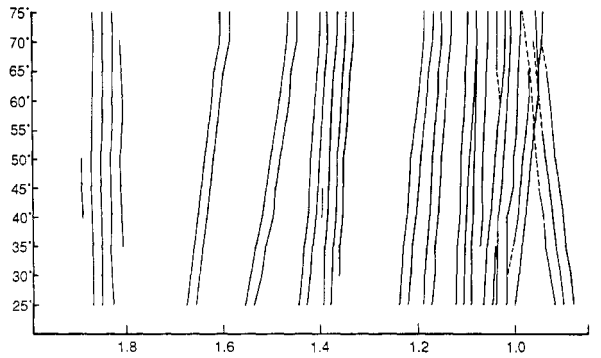

FIGURE 3: Temperature dependence in the methyl region of human β-endorphin in 60% CD_3OD–40% D_2O. At all temperatures the reference was the internal methanol peak at 3.30 ppm.

suggestive of a nonrandom structure in which a methyl group is upfield shifted, probably as a result of a ring current shift from a nearby tyrosine or phenylalanine. Starting from 25 °C, a temperature series was undertaken in steps of 5 °C up to 75 °C. The reference was chosen to be a tyrosine resonance set at 6.90 ppm.

In the aromatic region, one peak shows a gradual temperature dependence of its chemical shift: from 7.30 ppm at 25 °C to 7.255 ppm at 75 °C. The other peaks exhibit almost no temperature dependence or a slight upfield shift.

Figure 3 shows the shifts of the upfield methyl peaks, which are particularly easy to follow during this experiment. The temperature effect on these peaks is more pronounced than in the aromatic region. First, the lone upfield methyl shows a strong and steady *downfield* shift from 0.90 to 0.97 ppm. This temperature dependence is remarkable since the remainder of the peaks in this region all have a tendency to move *upfield*. In fact, many of the methyl peaks around 1.00 ppm decrease by 0.05 ppm in chemical shift between 25 and 75 °C. Further downfield, the doublets at 1.55 and 1.67 ppm at 25 °C move to 1.45 and 1.59 ppm, decreases of 0.10 and 0.08 ppm, respectively. In contrast, other peaks, e.g., at 1.85 ppm, remain very stable. This indicates significant differential temperature dependences of up to 0.17 ppm.

Such marked changes in the methyl region can be explained by changes in the peptide conformation. This interpretation is substantiated by marked changes in shape and distribution of the peaks in the α-CH region of the spectrum between 25 and 75 °C. In conclusion, this temperature experiment establishes that between 25 and 75 °C the β-endorphin undergoes a steady change in conformation. This is consistent with a nonrandom conformation of the neuropeptide at 25 °C.

To further characterize the structure in the water–methanol mixed solvent, we applied the two-dimensional NMR sequential assignment technique using COSY and NOESY experiments. This consists of three steps. First, the spin systems of amino acids are identified from side-chain to amide resonances. Second, the identified spin systems are ordered sequentially by using NOEs between backbone hydrogens of neighboring residues and then matched against the known primary sequence. This yields the assignments of the spin systems to specific residues. Third, the pattern of backbone NOEs can be interpreted in terms of α-helices or β-strands.

2-D Spin System Identification. Identification of the side chains relied primarily on COSY data, shown in Figure 4, complemented when ambiguities arose by NOESY connectivities between hydrogens that are four or five bonds removed, such as between α-CH and γ-CH_2 resonances. All side-chain systems were identified. Because of the downfield shift of the β-threonine resonance, the two alanines and three threonines

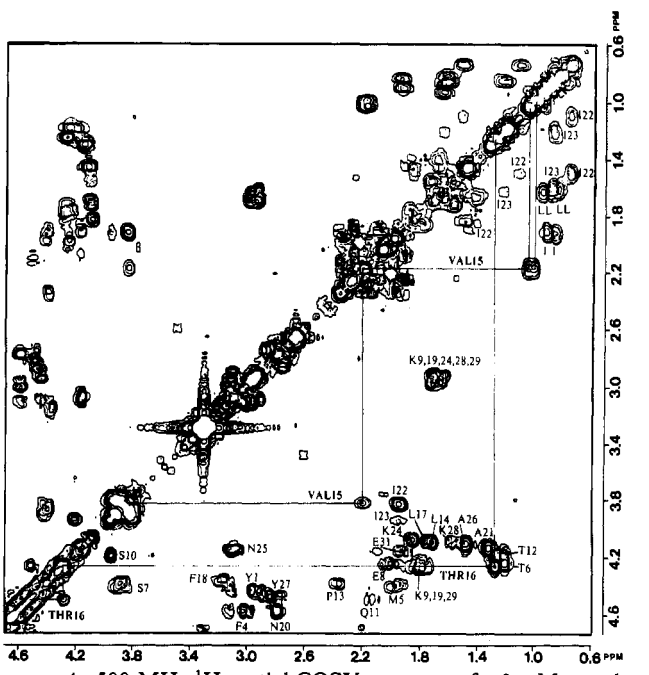

FIGURE 4: 500-MHz ^1H partial COSY spectrum of a 3 mM sample of human β-endorphin in a mixed solvent of 60% CD_3OD–40% D_2O at 23 °C, referenced to internal methanol set at 3.30 ppm. The spectrum was collected as described under Materials and Methods. This figure displays the assignments in the aliphatic region and the tracing of the connectivities from Val-15 and Thr-16.

were all characterized by COSY cross-peaks from the methyl region to the α-CH region. As expected, five such peaks were observed. The threonines are further distinguished by a β-CH to α-CH connectivity. Two of these are observed, and the third, ambiguous because it is too close to the diagonal, was independently observed by a NOESY cross-peak from the γ-CH_3 to α-CH. The two isoleucines were also readily identified from their distinctive COSY connectivity patterns, with the best aligned β-CH to α-CH cross-peak in agreement with the NOESY cross-peak from the γ-CH_3 to the α-CH resonances. The side chain of the single valine was assigned by tracing its double γ-CH_3 to β-CH to α-CH cross-peaks. The two leucine connectivity patterns were interrupted at the γ-CH to β-CH_2 because this cross-peak is in a region crowded by five lysines and because it is near the diagonal. Five possible β-CH_2 to α-CH peaks, with β-resonances close to the γ-resonance of the leucines, were picked as likely leucine connectivities. Two of these were tentatively chosen to be the leucine connectivities on the basis of intra-side-chain NOEs from the δ-methyl resonances to the α-CH. The evidence from these NOEs was considered to be weak, and the leucine spin-system identification was made final only after all the assignments were established to be consistent. The COSY connectivities of the five lysines side chains could be traced from ε-CH_2 to α-CH. Some ambiguity arose in distinguishing between eight possible β-CH_2 to α-CH cross-peaks, but five could be traced to the lysines, two to the leucines, and one to either proline, methionine, glutamate, or glutamine. This group of amino acids accounted for five residues with overlapping COSY cross-peaks and essentially similar connectivity patterns. At this stage they could not be distinguished and were referred to collectively as "X". This allowed identification of five β-CH_2 to α-CH cross-peaks from amino acids X. The two asparagines, two phenylalanines, and two tyrosines all lack a γ-resonance, and their six neighboring β-CH_2 to α-CH COSY cross-peaks were indistinguishable. Fortunately, NOESY cross-peaks to the β-CH peaks from the δ-NH_2 of one as-

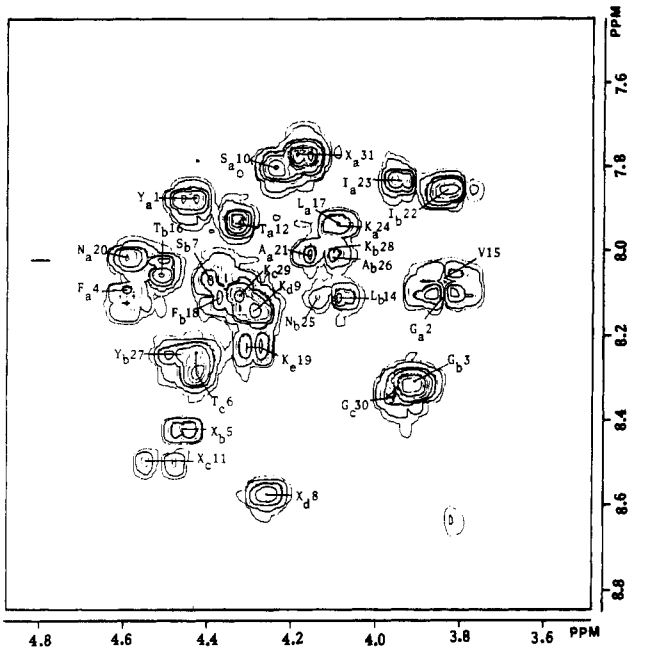

FIGURE 5: Assignments in the NH to α-CH region of the COSY spectrum of a 3 mM sample of human β-endorphin collected under the same conditions as Figure 4. The subscripts refer to the arbitrary nomenclature used in the text to distinguish prior to assignments between residues of the same amino acid type.

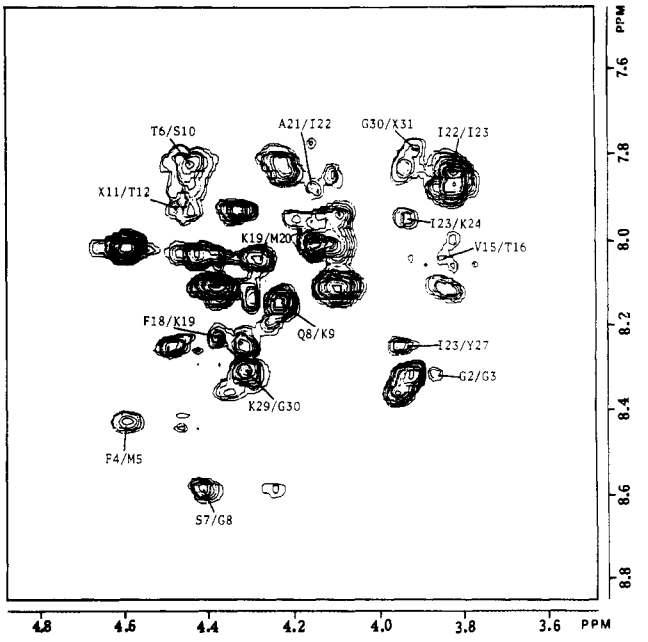

FIGURE 6: 500-MHz ^{1}H partial NOESY spectrum of human β-endorphin. The spectrum was collected in absolute value mode as described under Materials and Methods with a mixing time of 250 ms. The region shown is the same as in Figure 5, and the α-CH$_i$ to NH$_{i+1}$ connectivities are labeled.

paragine and from the δ-CH of one tyrosine and both phenylalanines allowed tracing of the side-chain connectivities of all except one tyrosine and one asparagine. The corresponding unidentified β to α connectivities were tentatively assigned by considering that the two β-CH$_2$ resonances of asparagine are often more equivalent than those of tyrosine. The remaining amino acids were two serines that were readily identified from their COSY cross-peak, as were three glycines with slightly inequivalent α-CH$_2$ resonances.

Extension of the spin-system identification to the amides was complicated by the overlap of the α-CH resonances and by the low resolution of the data: 8.4 Hz in F2 and 16.8 Hz in F1, leading to an associated error for every peak of $\pm$0.03 ppm. Starting with low α-CH chemical shifts, the α-CH to amide COSY connectivities, shown in Figure 5, were assigned as follows. The three glycines, two isoleucines, and Val-15 were considered as a group since they have close α-CH shifts. Two of the glycine cross-peaks were identified on the basis of their α-CH shift and evidence from a 2-D J-resolved experiment clearly showing two glycine triplet resonances at 8.32 and 8.08 ppm. From NOESY data, both the valine and the isoleucines were also identified. In the case of the valine, intra-side-chain NOEs between the amide and both the β- and γ-resonances were observed, and similar NOEs were also observed between the amide and side-chain resonances of the isoleucines. The third glycine cross-peak remained undetermined but must be close to either of the first two glycines since their α-resonances are close and since the absence of a third triplet in the 2-D J-resolved experiment suggested that the amide resonances of two glycines are superimposed.

The next group of α-CH to NH cross-peaks to identify extended from 4.09 to 4.21 ppm and corresponded to nine residues. Among these, unambiguous identification relying on intra amino acid NOEs could be made for both alanines (NH to γ-methyls NOEs), one leucine, and one asparagine (NH to β-CH$_2$). One X and one serine could then be matched from their α-resonance chemical shift to α-CH to NH cross-peaks by default. This left ambiguous amide shifts for three amino acids: one leucine (8.10 or 7.94 ppm) and two lysines (8.10, 8.01, or 7.94 ppm).

Further downfield, another X resonance amide was identified through an α to amide NOESY cross-peak. By default the following three amide to α-CH COSY connectivities were identified as lysines. A threonine and a phenylalanine followed and, for both, the α to amide connectivity could be identified from chemical shift alone and for threonine was also confirmed by a γ-CH$_3$ to amide NOE. In similar fashion, the next group of amino acids extended from 4.40 to 4.51 ppm and contained seven amino acids, two tyrosines, two Xs, two threonines, and one serine, which were to be matched to seven distinct α-CH to NH COSY cross-peaks. Again, NOEs allowed unambiguous identification of the amide resonances for all but one threonine and one X, but these were then matched by default to the two remaining COSY cross-peaks. The last two amino acids were an asparagine and a phenylalanine to be matched to two cross-peaks. With direct NOESY evidence (β-CH$_2$ to NH connectivity) for the asparagine amide identification, the phenylalanine was identified by default, which completed the spin-system identification procedure.

Sequential Assignments. The last step to complete the assignments was to identify each spin system in terms of a specific residue. This was done by analyzing the α-CH$_i$ to NH$_{i+1}$ and NH$_i$ to NH$_{i+1}$ NOESY connectivities, shown in Figures 6 and 7, respectively.

Tyr-1–Gly-2. There are two tyrosine spin systems, Ya and Yb, and three glycine systems, Ga, Gb, and Gc. Among six possible Tyr-1–Gly-2 combinations, there was no evidence of a NOESY cross-peak from α-CH to NH between Ya–Gb, Yb–Gb, Ya–Gc, Yb–Gc, and Yb–Ga. However, a weak cross-peak may have been present between Ya and Ga at 4.42, 8.11 ppm. Confirming evidence from the NH–NH NOESY spectrum revealed no connectivity between Ya and either Gb or Gc, nor between Yb and Ga, Gb, or Gc, as expected. But a strong cross-peak can be seen at 7.89, 8.12 ppm, which corresponded to the Ya NH resonance at 7.88 ppm and the Ga NH resonance at 8.10 ppm. Thus, both an α-CH$_i$–NH$_{i+1}$ and an NH$_i$–NH$_{i+1}$ were observed between Ya and Ga, and

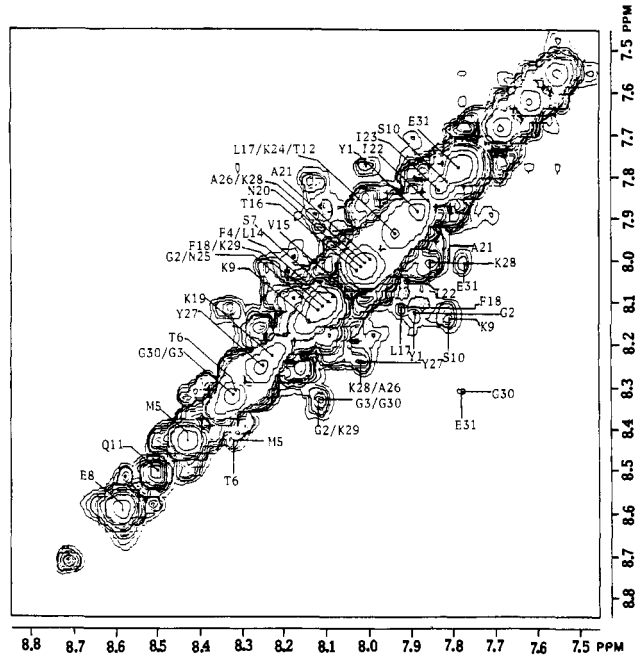

FIGURE 7: Same spectrum as in Figure 6, the NH–NH region. The NH_i to NH_{i+1} connectivities are displayed.

there is no evidence of similar connections between the other possible pairings of {Ya, Yb} and {Ga, Gb, Gc}. Accordingly, we assigned Tyr-1 at Ya and Gly-2 at Ga.

Gly-2–Gly-3. Gb and Gc have overlapping α-CH chemical shifts. Thus the NOESY α-CH to NH cross-peak could be either or both the intra- and interresidue cross-peaks of Gb, Gc, or between Gb and Gc. More helpful was the cross-peak at 3.86, 8.32 ppm from Ga to Gb. In the NH–NH region, there was no evidence that Gb and Gc or Ga and Gc are sequential, but a cross-peak existed at 8.11, 8.32 ppm. Coupled with the α-CH to NH at 3.86, 8.32 ppm mentioned above, it was the strongest possible evidence that Ga and Gb are sequential, in that order. Thus, Ga is assigned to Gly-2 and Gb to Gly-3. This independently confirmed the Tyr-1–Gly-2 assignment.

Gly-3–Phe-4. It was not possible to rule out any of the six possible glycine–phenylalanine combinations. The amide shifts of the phenylalanines were almost equal, and they were indistinguishable from an α-CH to NH connectivity. Also, while Ga could be connected to a phenylalanine residue through a peak at 8.11, 3.85 ppm, so could Gb and Gc with a possible NH–NH connectivity overlapping that from Gly-2 to Gly 3 at 8.10, 8.33 ppm. On the strength of the previous assignments, the best hypothesis kept Gly-3 at Gb with no conclusion about Phe-4.

Phe-4–Met-5. This assignment could be made on the strength of the very large 4.60, 8.43 ppm NOESY connectivity, which was most simply explained by Phe-4 being Fa and Met-5 being Xb. (Alternate explanations would invoke an α-CH to NH connectivity between Phe-4 and one of Glu-8, Gln-11, or Glu-31.)

Met-5–Thr-6. This assignment was made on the strength of the NOESY (8.43, 8.31 ppm) NH–NH connectivity, assuming that Met-5 is at Xb. Indeed, only Met-5 has an NH near 8.42 ppm, and the amide resonance at 8.31 must either be Phe-4 or Thr-6. With Phe-4 already assigned, it must be that Thr-6 is at Tc.

Thr-6–Ser-7. No Ta–Sa, Ta–Sb, Tb–Sb, and Tc–Sb α-CH_i to NH_{i+1} NOESY cross-peaks are observable. Though Tb–Sa and Tc–Sa connectivities could lie behind a vast cross-peak at 4.43, 7.82 ppm, these two NOEs were too ambiguous to attempt any assignment for this sequential connectivity.

Ser-7–Glu-8. There were no α_i to NH_{i+1} cross-peaks to Xb or Xc from either Sa or Sb. However, there was at 4.40, 8.59 ppm a strong NOE cross-peak that corresponded well with an Sb–Xd sequential assignment. Unfortunately, Ser-10–Gln-11 would also match this assignment equally well. Without more evidence, Sb–Xd remained undetermined between residues 7 and 8 or 10 and 11.

Glu-8–Lys-9. This connectivity was assigned through a large cross-peak at 4.24, 8.15 ppm. The only good matching α-CH's were Xd at 4.26 (/4.24) ppm and Sa at 4.21 ppm, while the lone possible NH shift was Kd at 8.14 ppm. Thus, this particular peak could only arise from an α to NH NOE from either Xd or Sa to Kd. The first possibility fit with the sequential assignment Xd–Kd, while the second could only be explained by a Ser-7–Lys-9 NOE, which required invoking a 3_{10} α-helical conformation—a less plausible argument. Therefore, the assignments were Glu-8 at Xd and Lys-9 at Kd. In turn, following the analysis of Ser-7–Glu-8, Xd at Glu-8 implied that Ser-7 was Sb.

Lys-9–Ser-10. There were no detectable cross-peaks from lysines to serines except at 4.26, 7.81 ppm where a "hidden" cross-peak could exist, buried in the overlap between its neighbors. This possibility was supported by a very strong NH–NH cross-peak at 8.14, 7.81 ppm. This pointed to Lys-9 at Kd and Ser-10 at Sa, thus confirming the previous Lys-9 assignment to Kd and strengthening the chain of evidence that put Ser-7 at Sb, a conclusion further reinforced by the assignment of Sa to Ser-10.

Ser-10–Gln-11. The analysis for this assignment is similar to that with Ser-7–Glu-8. However, with the benefit of having assigned the intervening residues, it was clear that Ser-10 must be at Sa, while Gln-11 remained undetermined between Xa and Xc since Sa had no NOESY links to these two unassigned X's.

Gln-11–Thr-12. Among all the possible X to threonine NOESY connectivities, the NOE (4.48, 7.93 ppm) from Xc to Ta has no simple alternative explanation other than Gln-11 is at Xc and Thr-12 at Ta.

Leu-14–Val-15. Both leucines had similar α-CH chemical shifts, at 4.10 and 4.11 ppm. In the absence of a NOESY NH–NH cross-peak, the assignment would have to be done through elimination once Leu-17 was assigned.

Val-15–Thr-16. Only one cross-peak was seen, at 3.84, 8.05 ppm, from the valine α resonance to the Tb amide. Thus it must be that Thr-16 is at Tb.

Thr-16–Leu-17. Tb–La, Ta–La, Tc–La, Ta–Lb, and Tc–Lb all may be alternate sequential assignments. In keeping with previous analysis, the most plausible assignment was Thr-16 at Tb and Leu-17 at La, which also implied, by default, that Leu-14 is at Lb.

Leu-17–Phe-18. Only La–Fa or La–Fb was consistent with an NH–NH cross-peak at 7.93, 8.11 ppm. Thus Leu-17 is at La, which confirmed the previous assignment, while Phe-18 could not be assigned unambiguously to Fa or Fb. However, previous assignment of Phe-4 to Fa left Fb to be Phe-18 by default.

Phe-18–Lys-19. This sequential assignment depended on the NOESY peak at 4.37, 8.23 ppm, which unambiguously arose between the relatively isolated Fb α-CH and the Ke NH. This consolidated the previous assignment of Phe-18 to Fb and put Lys-19 at Ke.

Lys-19–Asn-20. The large cross-peak at 4.28, 8.04 ppm (together with a possible 8.23, 8.02 ppm NH_i–NH_{i+1} connectivity) was very strong evidence that Ke and Na are se-

quential. No other K–N combination has a possible NH–NH cross-peak, and we concluded that Lys-19 was at Ke and Asn-20 was at Na.

Asn-20–Ala-21. No assignment could be made on the basis of this connectivity.

Ala-21–Ile-22. Both alanines have possible cross-peaks to Ib, via 4.14, 7.87 ppm, and Ia, via 4.10, 7.85 ppm, though the latter cross-peak was already invoked during the Leu-14–Val-15 assignment. However, the NH_i–NH_{i+1} cross-peak at 8.01, 7.86 ppm could correspond to either Aa or Ab, but only to Ib. Thus the sequential order must be Aa–Ib, leading to Ala-21 at Aa and Ile-22 at Ib.

Ile-22–Ile-23. Examination of the NOESY spectra showed that an α_i to NH_{i+1} cross-peak is more likely to be from Ib to Ia than from Ia to Ib. Thus, Ile-22 is at Ib and Ile-23 at Ia.

Ile-23–Lys-24. Ia could have connectivities to Ka (3.94, 7.95 ppm) or to Ke (3.94, 8.25 ppm). Neither of these possible assignments shows a corresponding NH_i–NH_{i+1} cross-peak. Ib can also have α-CH_i–NH_{i+1} connectivities to Kb and Kc, the latter possibly coupled with an NH_i–NH_{i+1} cross-peak. With so many ambiguities, this sequential assignment could only be done by arguing that the two very strong cross-peaks listed at the beginning could not be reasonably accounted for without requiring that Ile-23 be at Ia. This is in contrast to the Ib–K possible connections that do not involve new cross-peaks. Similarly, there was no good explanation for the Ia–Ka cross-peak other than being a sequential connectivity. On the other hand, the second cross-peak could be shown, below, to belong to an Ile-23–Tyr-27 connectivity. Thus the evidence pointed to Ile-23 at Ia and Lys-24 at Ka.

Lys-24–Asn-25. This combination has already been examined when Lys-19–Asn-20 was considered. The conclusions remain the same, but now consistency with previous assignments requires that Lys-24–Asn-25 be matched with Ka and Nb. Confidence in the correctness of the two K–N sequential assignments was enhanced by the fact that they are independent, mutually exclusive, and compatible with all other assignments.

Asn-25–Ala-26. Here again the analysis was similar to that of Asn-20–Ala-21, and only the consistency requirement permitted assignment of Asn-25 to Nb and Ala-26 to Ab with an associated NH_i–NH_{i+1} cross-peak at 8.10, 8.01 ppm.

Ala-26–Tyr-27. There were two possibilities for this assignment: Aa–Ya by way of 4.14, 7.87 ppm with no NH–NH cross-peak or Aa/Ab–Yb with no α-CH–NH cross-peak but with NH–NH connectivity at 8.01, 8.25 ppm. No clear choice could be made in this case, but since Tyr-1 had been assigned at Ya, the only consistent sequential assignment would be Ala-26 at Ab and Tyr-27 at Yb. This was the only possibility that was also consistent with an observed cross-peak at 3.94, 8.25 ppm, interpreted as an Ile-23–Tyr-27 α-CH_i–NH_{i+4} connectivity.

Tyr-27–Lys-28. Ya/Yb–Ka/Kb were viable alternatives as is Ya–Kc. As NH–NH cross-peaks also existed for Ya/Yb–Kb, these last two were the favored matching assignments, definitely requiring that Lys-28 be at Kb. Tyr-27 was left at Yb for consistency.

Lys-28–Lys-29. Starting from Kb, which had been associated with Lys-28, the only possibility for Lys-29 was Kc (Ka was already assigned to Lys-19). This choice could correspond to the NH–NH cross-peak at 8.01, 8.10 ppm. While this assignment was weak in itself, it was consistent with prior analysis and as shown below fit with the remaining assignments.

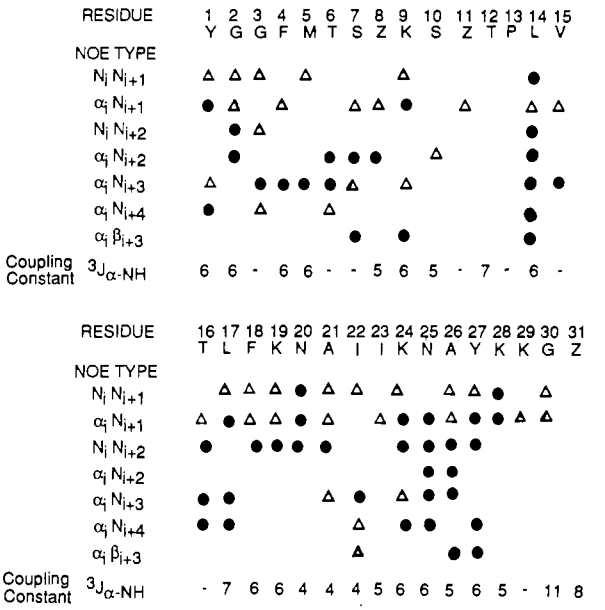

FIGURE 8: Summary of the sequential connectivities and coupling constants for human β-endorphin in 60% CD_3OD–40% D_2O at 23 °C. The NOEs were classified as unambiguous (△) when the associated peaks were well resolved and as ambiguous (●) if they had significant overlap with neighboring peaks. Each dot or triangle indicates the position of the ith residue. The coupling constants are in hertz with a precision of ±1 Hz.

Lys-29–Gly-30. This assignment was given away by the unambiguous cross-peak at 4.32, 8.32 ppm, which could only be explained by a Kc α-CH in proximity to a Gb/Gc amide. (The only other amide candidate was Thr-6, Thr-12, Thr-16 at Tc, which was not a reasonable hypothesis for Thr-12 and -16 since they have no neighboring X's and which for Thr-6 is incompatible with current assignments.) This left Lys-29 at Kc and Gly-30 at Gc/Gb.

Gly-30–Glu-31. This assignment could only be consistent with Gb/Gc–Xa, as determined by the cross-peak at 3.92, 7.79 ppm. Furthermore, an NH_i–NH_{i+1} existed at 8.32, 7.79 ppm, clearly connecting the Gly-30 and Glu-31 amides. Thus we obtained as our final sequential assignment Gly-30 at Gb/Gc and Glu-31 at Xa.

These 28 sequential assignments led to a complete determination of the β-endorphin spectrum in the 60% methanol–40% water solvent. The results are compiled in Table I.

Secondary Structure. Figure 8 summarizes the NOESY connectivities observed in the endorphin. Two distinct segments stand out: from Tyr-1 to Thr-12 and from Leu-14 to Tyr-27. Both are characterized by many observable or possible α_i to NH_{i+3} and α_i to NH_{i+4} NOEs. These two stretches have no NOE connectivities between them and are separated by a proline at residue 13. The type of NOEs within both segments 1 and 2 strongly supports the presence of an α-helix as characterized by three types of connectivities: NH_i to NH_{i+1}, α-CH_i to NH_{i+3}, and α-CH_i to NH_{i+4} (Wüthrich et al., 1984) and by small $^3J_{\alpha\text{-NH}}$ coupling constant values (Pardi et al., 1984).

Segment 1 starts with three consecutive NH_i–NH_{i+1} connectivities followed by another one between residues 5 and 6. There are also, between residues 1 and 10, two α-CH_i–NH_{i+4} NOEs, three α-CH_i–NH_{i+3} NOEs, and one α-CH_i–NH_{i+2} NOE, all observed with certainty. Eight possible additional NOEs also exist, four α-CH_i–NH_{i+3} and four α-CH_i–NH_{i+2} as shown in Figure 8. Altogether, these NOEs are strong evidence that an α-helix starts at residue 1 and extends to residue 12. Finally, the $J_{\alpha\text{-NH}}$ coupling constants are equal

Table I: Complete Assignments in the Human β-Endorphin in a Mixed 40% Water–60% Methanol Solvent[a]

amino acid	NH	α-CH	β-CH	others
Tyr-1	7.88	4.42	2.94	δ-CH 7.25
				ε-CH 6.81 or 6.75
Gly-2	8.11	3.86		
Gly-3	8.32	3.91		
Phe-4	8.10	4.60	2.97/3.11	δ-CH 7.25
				ε-CH 7.20–7.33
				ζ-CH 7.20–7.33
Met-5	8.43	4.43	1.96	γ-CH_2 2.34?
Thr-6	8.31	4.41	4.26	γ-CH_3 1.20
Ser-7	8.08	4.40	3.89	
Glu-8	8.59	4.24	2.01	γ-CH_2 2.16?
Lys-9	8.15	4.27	1.86–1.72	γ-CH_2 1.57, 1.52, or 1.45
				δ-CH_2 1.73–1.64
				ε-CH_2 2.93–3.00
Ser-10	7.81	4.21	3.95	
Gln-11	8.50	4.49	2.13	γ-CH_2 2.37 or 2.78?
				ε-NH_2 7.55/6.82
Thr-12	7.94	4.32	4.19	γ-CH_3 1.21
Pro-13		4.39	2.36	γ-CH_2 2.05?
				δ-CH_2 2.47?
Leu-14	8.10	4.11	1.72	γ-CH 1.64 or 1.63
				δ-CH_3 0.95/0.89 or 0.89/0.84
Val-15	8.06	3.83	2.20	γ-CH_3 1.03
Thr-16	8.06	4.50	4.28	γ-CH_3 1.27
Leu-17	7.93	4.10	1.77	γ-CH 1.63 or 1.64
				δ-CH 0.95/0.89 or 0.89/0.84
Phe-18	8.11	4.36	3.16	δ-CH 7.25
				ε-CH 7.20–7.33
				ζ-CH 7.20–7.33
Lys-19	8.23	4.30/4.27	1.86–1.72	γ-CH_2 1.57, 1.52, or 1.45
				δ-CH_2 1.73-1.64
				ζ-CH_2 2.93–3.00
Asn-20	8.04	4.59	2.80	δ-NH_2 7.69/6.95
Ala-21	8.00	4.14	1.32	
Ile-22	7.86	3.83	1.95	γ-CH_3 1.11
				γ-CH_2 1.52
				γ-CH_3 0.86 or 0.92
				δ-CH_3 0.75
Ile-23	7.84	3.95	1.95	γ-CH_3 1.22
				γ-CH_2 1.66
				γ-CH_3 0.92 or 0.86
				δ-CH_3 0.87
Lys-24	7.95	4.09	1.85	γ-CH_2 1.52 or 1.45
				δ-CH_2 1.73–1.64
				ε-CH_2 2.43–3.00
Asn-25	8.12	4.15	3.09	δ-NH_2 7.60–6.90
Ala-26	8.01	4.10	1.49	
Tyr-27	8.25	4.48	2.85/2.77	δ-CH 7.15
				ε-CH 6.75 or 6.81
Lys-28	8.01	4.10	1.58	γ-CH_2 1.48
				δ-CH_2 1.68
				ε-CH_2 2.93–3.00
Lys-29	8.11	4.32	1.86–1.72	γ-CH_2 1.57, 1.52, or 1.45
				δ-CH_2 1.73–1.64
				ε-CH_2 2.93–3.00
Gly-30	8.32	3.92		
Glu-31	7.79	4.18	2.10/1.92	γ-CH_2 2.27?

[a] Chemical shifts are referenced to internal methyl alcohol set at 3.30 ppm and are accurate to ±0.03 ppm. Question marks indicate tentative assignments.

to or less than 6 Hz, also in good agreement with a helix in segment 1.

Segment 2, from Leu-14 to Tyr-27, is characterized by 16 α-CH_i–NH_{i+3} and α-CH_i–NH_{i+4} connectivities with only Phe-18, Asn-20, and Ile-23 presenting neither. Also, NH_i–NH_{i+1} NOEs occur in a continuous stretch of six residues from Leu-17 to Ile-22 and are absent in only four residues, Val-15, Thr-16, Ile-23, and Asn-25. Except for Leu-17 at 7 Hz, the coupling constants $^3J_{\alpha\text{-NH}}$ are smaller than or equal to 6 Hz, in support of a helix.

This evidence establishes the presence of an α-helix in segment 2. The sequence of NH_i–NH_{i+1} NOEs and the perfect $^3J_{\alpha\text{-NH}}$ values of residues 20, 21, and 22 indicate a stable helical core encompassing residues 17–22. Four possible α-CH_i–NH_{i+3} NOEs and three possible α-CH_i–NH_{i+4} NOEs in the stretch Leu-14–Val-15–Thr-16–Leu-17 suggest strongly that the α-helix starts immediately at Leu-14. Unfortunately, the Val-15 and Thr-16 $^3J_{\alpha\text{-NH}}$ cannot be measured, and NH_i–NH_{i+1} NOEs cannot be detected for these two residues.

The helix end is more difficult to pinpoint. An α-CH_i–NH_{i+3} NOE is observed at Lys-24 and two more possibly occur at Asn-25 and Ala-26. Two possible α-CH_i–NH_{i+4} NOEs could exist also at Lys-24 and Asn-25. Small $^3J_{\alpha\text{-NH}}$ values occur until Lys-28 and NH_i–NH_{i+1} connectivities are seen at Lys-24, Ala-26, and Tyr-27 and possibly at Lys-28. This evidence is compatible with the α-helix extending to Lys-28 or Lys-29.

The final stretch from Lys-28 to Glu-31 is characterized by one extreme value of $^3J_{\alpha\text{-NH}}$, 11 Hz at Gly-30, and by a large NOE at 7.77, 8.01 ppm between the amide hydrogens of Lys-28 and Glu-31. This is evidence for a restrained conformation at the C-terminus that brings Lys-28 and Glu-31 into proximity, possibly forming a salt bridge.

Discussion

Many studies of the secondary structure of β-endorphin have been undertaken, pointing either to a random coil or to the possible existence of a tertiary structure in aqueous solutions and to a high percentage of helix formation in mixed water–organic solvent solutions, with conflicting proposals for the helix location(s). Since current techniques of two-dimensional NMR spectroscopy allow the definition of the secondary structure of small proteins (Wemmer et al., 1986; Klevit & Waygood, 1986; Holak & Prestegard, 1986), we attempted to resolve these questions.

Our results are consistent with and allow us to explain the results of previous workers. In water (Hollosi et al., 1977; Yang et al., 1977) CD measurements did not reveal any significant amount of secondary structure, and hydrodynamic measurements indicated an extended noncompact structure consistent with little tertiary structure. Similarly, the NMR temperature experiments failed to reveal any significant spectral alteration between 24 and 75 °C, establishing that the endorphin is in a random-coil conformation in water.

In a 40% water–60% methanol mixed solvent, the temperature experiments show a slow noncooperative transition between two conformations. The starting conformation in this transition is characterized by two helical segments between residues 1 and 12 and between residues 14 and 28, characterized by numerous α-CH_i–NH_{i+2}, α-CH_i–NH_{i+3}, and α-CH_i–NH_{i+4} NOEs. These NOEs were classified as unambiguous when they were well resolved or as ambiguous if they had extensive overlap with neighboring crosspeaks. The helices are especially well established by unambiguous NOEs between Tyr-1 and Ser-10 and between Leu-14 and Lys-28. Between Ser-10 and Thr-12, the NOE evidence for a helix is scarcer and relies on one unambiguous α-CH_i–NH_{i+3} NOE at Lys-9. This NOE does suggest that the helix extends to Thr-12, but the lack of additional supporting evidence makes it difficult to find an exact helix cutoff. This may reflect fraying of the helix as it deviates gradually from perfect helicity.

The second helix is especially well characterized between residues 14 and 20 and between residues 22 and 30. Evidence that these segments are part of a single helix comes from the stretch of NOEs between successive amide hydrogens between residues 17 and 22 and from the low $^3J_{\alpha\text{-NH}}$ coupling constants

at residues 20, 21, and 22. Also, the most simple explanation of the temperature-induced transition of the 0.75 ppm resonance is a ring current shift at Ile-22 due to Phe-18, as these two residues are brought into proximity by the formation of an α-helix.

Thus NMR establishes that methanol induces formation of helices between residues 1 and 12 and 14 and 28, with a turn between residues 28 and 31. This determines precisely the location and extent of the helical conformation detected in methanol by Yang et al. (1977) and Jibson and Li (1981). It is likely but not established that the trifluoroethanol-induced helices occur in the same regions. The presence of a turn at the C-terminus is in agreement with the work of Hammonds et al. (1982), specifically, his observation that the complete β-endorphin is relatively less helical than the fragment extending from residue 1 to 27. However, this confirming evidence is weak, given the margin of error in CD measurements on small peptides.

It is interesting to note that the formation of both helix segments occurs at sites considered critical to binding (Li, 1982). While it is not clear that the secondary structure of human β-endorphin in a water–methanol mixed solvent is a good approximation to the in vivo conformation, Hammonds and his colleagues (1982) showed a correlation between helix-forming potential of β-endorphin fragments and binding to rat brain membrane. This suggests that helix formation between residues 1 and 10 and between 14 and 28 plays a role in the binding affinity of β-endorphin to the opioid receptors. The absence of long-range NOEs between distant residues prevented investigating the tertiary structure of the peptide. This may indicate that the helical segments of β-endorphin are flexible with respect to each other and that their relative orientation will be strongly influenced by the receptor itself.

ACKNOWLEDGMENTS

We thank Dr. Andrew Lane for helpful discussions and suggestions during the course of this work, Daniel Sze for his comments on the draft, and Robin Holbrook for her assistance in the preparation of the manuscript.

Registry No. Human β-endorphin, 61214-51-5.

REFERENCES

Anil-Kumar, Ernst, R. R., & Wüthrich, K. (1980) *Biochem. Biophys. Res. Commun. 95*, 1–6.

Aue, W. P., Bartholdi, E., & Ernst, R. R. (1976a) *J. Chem. Phys. 64*, 2229–2246.

Aue, W. P., Karhan, J., & Ernst, R. R. (1976b) *J. Chem. Phys. 64*, 4226.

Bax, A., & Freeman, R. (1981) *J. Magn. Reson. 44*, 542–561.

Bewley, T. A., & Li, C. H. (1983) *Biochemistry 22*, 2671–2675.

Bewley, T. A., & Li, C. H. (1985) *Biochemistry 24*, 6568–6571.

Billeter, M., Braun, W., & Wüthrich, K. (1982) *J. Mol. Biol. 155*, 321–346.

Blanc, J., & Kaiser, E. T. (1984) *J. Biol. Chem. 259*, 9549–9556.

Blanc, J., Miller, R. J., & Kaiser, E. T. (1983) *J. Biol. Chem. 258*, 8277–8284.

Cabassi, F., & Zetta, L. (1982) *Int. J. Pept. Protein Res. 20*, 154–158.

De Marco, A., Zetta, L., & Kaptein, R. (1985) *Eur. Biophys. J. 11*, 187–193.

Gariepy, J., Lane, A. N., Frayman, F., Wilbur, D., Robien, W., Schoolnik, C. K., & Jardetzky, O. (1986) *Biochemistry 25*, 7854–7866.

Goldstein, A., Tachibana, S., Lowney, L. I., Hunkapillar, L. I., & Hood, L. (1979) *Proc. Natl. Acad. Sci. U.S.A. 76*, 6666–6670.

Graf, L., Hollosi, M., Patthy, A., Berzetei, I., & Ronai, A. (1980) *Neuropeptides 1*, 45–91.

Hammonds, R. G., Hammonds, A. S., Ling, N., & Puett, D. (1982) *J. Biol. Chem. 257*, 2990–2995.

Holak, T. A., & Prestegard, J. H. (1986) *Biochemistry 25*, 5760–5774.

Hollosi, M., Kajtar, M., & Graf, L. (1977) *FEBS Lett. 74*, 185–189.

Hughes, J., Smith, T. W., Kosterlitz, H. W., Fothergill, L. A., Morgan, B. A., & Morris, *Nature (London) 258*, 577–579.

Jardetzky, O., & Roberts, G. C. K. (1981) *NMR in Molecular Biology*, Academic, New York.

Jeener, J., Meier, B. H., Bachmann, P., & Ernst, R. R. (1979) *J. Chem. Phys. 71*, 4546–4553.

Jibson, M. D., & Li, C. H. (1981) *Int. J. Pept. Protein Res. 18*, 297–301.

Kaiser, E. T., & Kezdy, F. J. (1984) *Science (Washington, D.C.) 223*, 249–255.

Klevit, R. E., & Waygood, E. B. (1986) *Biochemistry 25*, 7774–7781.

Kline, A. D., & Wüthrich, K. (1985) *J. Mol. Biol. 183*, 503–507.

Kosterlitz, H. W. (1985) *Proc. R. Soc. London, B 225*, 27–40.

Li, C. H. (1964) *Nature (London) 201*, 924.

Li, C. H. (1982) *Cell (Cambridge, Mass.) 31*, 504–505.

Li, C. H., Yamashiro, D., Tseng, L.-F., & Loh, H. H. (1977) *J. Med. Chem. 20*, 325–328.

Nagayama, K., Anil-Kumar, Wüthrich, K., & Ernst, R. R. (1980) *J. Magn. Reson. 40*, 321–334.

Pardi, A., Billeter, M., & Wüthrich, K. (1984) *J. Mol. Biol. 180*, 741–751.

Schulz, R., Wuster, M., & Herz, A. (1981) *J. Pharmacol. Exp. Ther. 216*, 604–606.

Simon, E. J. (1982) *Ann. N.Y. Acad. Sci. 398*, 327–339.

Smith, A. P., & Loh, H. H. (1981) in *Hormonal Proteins and Peptides* (Li, C. H., Ed.) Academic, New York.

Taylor, J. W., Miller, R. J., & Kaiser, E. T. (1981) *J. Am. Chem. Soc. 103*, 6965–6966.

Taylor, J. W., Miller, R. J., & Kaiser, E. T. (1982) *Mol. Pharmacol. 22*, 657–666.

Taylor, J. W., Miller, R. J., & Kaiser, E. T. (1983) *J. Biol. Chem. 258*, 4464–4471.

Wagner, G., Anil-Kumar, & Wüthrich, K. (1981) *Eur. J. Biochem. 114*, 375–384.

Wemmer, D. E., & Kallenbach, N. R. (1983) *Biochemistry 22*, 1901–1906.

Wemmer, D. E., Kumar, V. N., Metrione, R. M., Lazdunski, M., Drobny, G., & Kallenbach, N. (1986) *Biochemistry 25*, 6842–6849.

Wider, G., Macura, S., Anil-Kumar, Ernst, R. R., & Wüthrich, K. (1984) *J. Magn. Reson. 56*, 207–234.

Williamson, M. P., Marion, D., & Wüthrich, K. (1984) *J. Mol. Biol. 173*, 341–360.

Wu, C. C. S., Lee, N. M., Loh, H. H., Yang, J. T., & Li, C. H. (1979) *Proc. Natl. Acad. Sci. U.S.A. 76*, 3656–3659.

Wuster, M., Schulz, R., & Herz, A. (1979) *Neurosci. Lett. 15*, 193–198.

Wuster, M., Schulz, R., & Herz, A. (1980) *Life Sci. 27*, 163–170.

Wüthrich, K., Wider, G., Wagner, G., & Braun, W. (1982) *J. Mol. Biol. 155*, 311–319.
Wüthrich, K., Billeter, M., & Braun, W. (1984) *J. Mol. Biol. 180*, 715–740.
Yang, J. T., Bewley, T. A., Chen, G. C., & Li, C. H. (1977) *Proc. Natl. Acad. Sci. U.S.A. 74*, 3235–3238.
Zetta, L., Kaptein, R., & Hore, P. J. (1982) *FEBS Lett. 145*, 277–280.
Zetta, L., Hore, P. J., & Kaptein, R. (1983) *Eur. J. Biochem. 134*, 371–376.
Zuiderweg, E. R. P., Kaptein, R., & Wüthrich, K. (1983) *Eur. J. Biochem. 80*, 5837–5841.

Nucleotide Interconversions in Microtubule Protein Preparations, a Significant Complication for Accurate Measurement of GTP Hydrolysis in the Presence of Adenosine 5′-(β,γ-Imidotriphosphate)

Janendra K. Batra, Chii M. Lin, and Ernest Hamel*

Laboratory of Pharmacology and Experimental Therapeutics, Developmental Therapeutics Program, Division of Cancer Treatment, National Cancer Institute, National Institutes of Health, Bethesda, Maryland 20892

Received December 18, 1986; Revised Manuscript Received April 7, 1987

ABSTRACT: Pursuing the observation of Carlier and Pantaloni [Carlier, M.-F., & Pantaloni, D. (1982) *Biochemistry 21*, 1215–1224] that adenosine 5′-(β,γ-imidotriphosphate) (pNHppA) strongly inhibited tubulin-independent phosphatases in microtubule protein preparations, we observed with a number of commercial preparations of pNHppA that a major proportion of the terminal phosphate of [γ-^{32}P]GTP added to microtubule protein preparations was rapidly converted into ATP. Initially postulating degradation of pNHppA to AMP followed by stepwise conversion of AMP to ATP, we isolated two nucleoside monophosphate kinase activities from microtubule protein capable of generating ATP from AMP + GTP. The amounts of these enzymes in microtubule protein preparations, however, are probably too low to account for rapid ATP formation. Instead, ATP formation most likely is caused by nucleoside diphosphate kinase acting on ADP contaminating commercial pNHppA preparations. Such ADP contamination was demonstrated by high-performance liquid chromatography, with the amount of ATP formed with different pNHppA preparations proportional to the amount of ADP contamination. Repurification of commercial pNHppA until it was free of contaminating ADP also resulted in the elimination of ATP formation. The repurified pNHppA potently inhibited GTP hydrolysis in microtubule protein preparations. In addition, especially when supplemented with equimolar Mg^{2+}, the repurified pNHppA strongly inhibited GTP hydrolysis and microtubule assembly in reaction mixtures containing purified tubulin and heat-treated microtubule-associated proteins (which contain negligible amounts of tubulin-independent phosphatase activity). We conclude that studies of microtubule-dependent GTP hydrolysis which make use of pNHppA must be interpreted with extreme caution.

Microtubule assembly generally requires GTP hydrolysis in amounts approximately stoichiometric with the amount of tubulin incorporated into polymer (MacNeal & Purich, 1978; Caplow & Zeeberg, 1980; Carlier & Pantaloni, 1982; Hamel et al., 1984). This GTP is located at the exchangeable nucleotide binding site of tubulin, for the equimolar amount of nonexchangeable GTP bound to the protein is unaltered during in vitro polymerization (Penningroth & Kirschner, 1977; Hamel et al., 1984) and may even persist without change in cellular microtubules (Spiegelman et al., 1977). Although many intriguing suggestions have been made to give GTP hydrolysis a more precise role in the assembly reaction or in the stabilization of microtubules [e.g., Kirschner (1980), Weisenberg (1980), Cote and Borisy (1981), Bonne and Pantaloni (1982), Carlier and Pantaloni (1982), Hill and Chen (1984), and Caplow and Reid (1985)], a severe limitation in the interpretation of data presented to support these ideas lies in the multiple enzyme contaminants found in microtubule protein preparations. These include nonspecific phosphatases which will degrade virtually any nucleotide, nucleoside diphosphate kinase, and adenylate kinase (Gaskin et al., 1974; Piras & Piras, 1977; Sutherland, 1976; Penningroth & Kirschner, 1977; Nickerson & Wells, 1978; Carlier & Pantaloni, 1982).

The phosphatases, in particular, by degrading GTP simultaneously and at a much faster rate than assembly-dependent GTP hydrolysis, obscure the reaction dependent on microtubule assembly. Carlier and Pantaloni (1982) demonstrated that the ATP analogue pNHppA,[1] supplemented by a molar equivalent of Mg^{2+}, markedly inhibited generation of P_i from GTP in preparations of microtubule protein. Assuming that the nonspecific phosphatases were virtually totally inhibited, that microtubule assembly and its associated GTP hydrolysis was unaffected by the high concentrations of either pNHppA or Mg^{2+} added to the reaction mixture, and that no

* Address correspondence to this author.

[1] Abbreviations: pNHppA, adenosine 5′-(β,γ-imidotriphosphate); MAP(s), microtubule-associated protein(s) (for the purposes of this study, a MAP is defined as any protein other than tubulin present in two-cycle microtubule protein preparations); Mes, 4-morpholineethanesulfonate; PEI–cellulose, poly(ethylenimine)–cellulose; TEAB, triethylammonium bicarbonate; NH_2ppA, adenylyl phosphoramidate; Pipes, 1,4-piperazinediethanesulfonate; P_i, inorganic phosphate.